

1 TITLE: Can MRI differentiate between ring-enhancing gliomas and intra-axial abscesses?

2

3 AUTHORS: Andrea Carloni^a, Marco Bernardini^{a,b}, Chiara Mattei^a, Angela Vittoria De

4 Magistris^a, Francisco Llabres-Diaz^c, Jonathan Williams^d, Rodrigo Gutierrez-Quintana^e, Anna

5 Oevermann^f, Daniela Schweizer-Gorgas^f, Cyrielle Finck^g, Isabelle Masseur^g, Valentina

6 Lorenzo^h, Annalisa Sabatiniⁱ, Barbara Contiero^b, Swan Specchi^a

7

8 AFFILIATIONS:

9 ^aDiagnostic Imaging department, Veterinary Hospital “I Portoni Rossi” Anicura Italy, Zola

10 Predosa (BO), Italy.

11 ^bDepartment of Animal Medicine, Production and Health, Clinical Section, University of

12 Padua, Legnaro, Padua, Italy.

13 ^cDepartment of Clinical Science and Services, Royal Veterinary College, Hatfield, UK

14 ^dPathobiology and Population Sciences, Royal Veterinary College, Hatfield, UK

15 ^eSchool of Veterinary Medicine, College of Medical Veterinary and Life Sciences, University

16 of Glasgow, UK.

17 ^fDivision of Neurological Sciences, Vetsuisse Faculty, University of Bern, Bern, Switzerland.

18 ^gDepartment of Clinical Sciences, Faculty of Veterinary Medicine, University of Montreal,

19 Saint-Hyacinthe, Qc, Canada.

20 ^hNeurología Veterinaria, Getafe, Madrid, Spain.

21 ⁱVeterinary Hospital “Gregorio VII”, Roma, Italy.

22

23 CORRESPONDENCE: swan.specchi@anicura.it

24

25 KEYWORDS: brain; neoplasia; infection; dog; cat;

26

27 CONFLICT OF INTEREST DISCLOSURE: The authors have no conflict of interest to
28 declare.

29

30 PRESENTATION DISCLOSURE: The preliminary results of this manuscript have been
31 presented at the online 2021 Annual EVDI Conference.

32

33 EQUATOR NETWORK DISCLOSURE: Relevant details described in the Strobe Vet-
34 statement checklist were included in this manuscript.

35 ABSTRACT

36 Gliomas of the brain may appear as expansile ring-enhancing masses in magnetic resonance
37 imaging (MRI) studies, mimicking the appearance of intra-axial abscesses. The aims of this
38 study were to compare the MRI features of ring-enhancing gliomas and intra-axial brain
39 abscesses in dogs and cats and to identify the characteristics that might help differentiate
40 them. For this multicenter, retrospective, and observational study, inclusion criteria were the
41 following: a) a definitive diagnosis of glioma or abscess based on cytological or
42 histopathological examination following CSF collection or surgical biopsy/necropsy,
43 respectively; b) MRI study performed with a high or low field MRI scanner, including a same
44 plane T1W pre- and post-contrast, a T2W and a T2 FLAIR sequence in at least one plane. If
45 available, delayed T1W post-contrast, T2*W GE, DWI/ADC and SWI sequences were also
46 evaluated. Sixteen patients were diagnosed with ring-enhancing gliomas and 15 with intra-
47 axial abscesses. A homogenous signal on T1W ($P = 0.049$) and T2W ($P = 0.042$) sequences, a
48 T2W ($P = 0.005$) or T2*W GE ($P = 0.046$) peripheral hypointense halo and an even
49 enhancing capsule ($P = 0.002$) were significantly associated with brain abscesses. A
50 progressive central enhancement on delayed T1W post-contrast sequences was correlated
51 with ring-enhancing gliomas ($P = 0.009$). The combination of the following features was
52 suggestive of brain abscess: homogeneous T1W or T2W signal intensity, a T2W or T2*W GE
53 peripheral hypointense halo and an evenly enhancing capsule. Central progression of
54 enhancement on delayed T1W post-contrast sequences was suggestive of glioma.

55 INTRODUCTION

56 Gliomas are primary neuroepithelial tumors accounting for approximately 35–37% of all
57 primary brain tumors in dogs.^{1,2} Glial tumors are less common in cats, representing
58 approximately 8% of feline primary brain tumors.³ Commonly reported MRI features of
59 gliomas have included single, intra-axial, T1-weighted (T1W) iso- to hypointense and T2-
60 weighted (T2W) iso- to hyperintense to normal brain parenchyma lesions, with cyst-like or
61 necrotic areas and variable distribution and degree of contrast enhancement.^{1,4-7} An
62 intratumoral hemorrhagic component has also been reported.⁶ Brain abscesses are uncommon
63 in companion animals and may develop via a hematogenous spread of bacteria, direct
64 invasion/contiguity, or contamination of cerebrospinal fluid.⁸⁻¹⁵ A brain abscess originates as
65 a localized area of neutrophilic cerebritis which, if untreated, may progress into liquefactive
66 necrosis containing viable and degenerate neutrophils (pus) surrounded within 1 to 2 weeks
67 by a well-vascularized fibrovascular capsule.^{8,9} On MRI, a brain abscess has been reported as
68 a focal, T2W hyperintense and T1W hypointense lesion compared to normal brain
69 parenchyma, with a necrotic non-enhancing center, surrounded by a thick and strongly
70 contrast-enhancing peripheral rim.^{11-13,15,16}

71 A recent review in the veterinary literature reports up to 45% of gliomas having partial or
72 complete ring-enhancement;¹⁷ therefore, gliomas may appear as expansile ring-enhancing
73 masses, mimicking the radiological appearance of intra-axial abscesses.¹⁸ In human medicine,
74 multiple MRI studies using specific sequences have attempted to find unique characteristics
75 to distinguish between ring-enhancing gliomas and abscesses. A hypointense peripheral
76 capsule on T2W images caused by paramagnetic free radicals within phagocytic
77 macrophages, often associated with susceptibility artifact in T2W gradient echo (T2*) and
78 with a “double rim sign” in susceptibility-weighted imaging (SWI), is considered a
79 distinguishing feature of brain abscesses in humans.^{19,20} Abscesses commonly show restricted

80 diffusion in diffusion weighted imaging (DWI) while gliomas usually do not.^{18, 21-23} However,
81 overlapping imaging features have been reported.²⁴⁻²⁶ Since the two diseases require very
82 different treatment and have a different prognosis, a correct imaging interpretation is
83 paramount.^{13,17,27,28}

84 The aims of the current study were to compare the MRI features of confirmed ring-enhancing
85 gliomas and intra-axial brain abscesses in dogs and cats and to identify the imaging features
86 that might help to differentiate them. Authors hypotheses were 1) some MRI qualitative
87 characteristics would be associated with brain abscess/glioma classification and, 2) a
88 threshold value for the ratio between lesion diameter and capsule thickness in T1W post-
89 contrast sequences could be used as a cut-off for discriminating between brain abscesses and
90 gliomas.

91

92 **MATERIALS AND METHODS**

93 **CASE SELECTION CRITERIA**

94 This was a multicenter, retrospective, observational study. All animals included were client-
95 owned and underwent MRI examinations of the brain as part of their clinical workup.

96 Previous informed written consent was obtained from all dog owners. All the procedures
97 performed complied with the European legislation “on the protection of animals used for
98 scientific purposes” (Directive 2010/63/EU).

99 The databases of the Veterinary Hospital “I Portoni Rossi” Anicura Italy, the Veterinary
100 Teaching Hospital of the University of Bern, the Royal Veterinary College, the University of
101 Glasgow, the University of Montreal, the Veterinary Clinic “Neurología Veterinaria” and the
102 Veterinary Hospital “Gregorio VII” were searched for dogs and cats diagnosed with a single
103 ring-enhancing intra-axial lesion. All hospitals approved the use of their imaging data for this
104 project.

105

106 Inclusion criteria for this study were the following: (1) a definitive diagnosis of glioma or
107 abscess based on cytological or histopathological examination following CSF collection or
108 surgical biopsy/necropsy, respectively; (2) a MRI study performed with a high or low field
109 MRI scanner, including at least a same plane pre- and postcontrast T1W and a T2W sequence
110 in at least one plane as well as a T2 FLAIR sequence in any plane. If available, T2*W GE,
111 DWI/ADC, SWI and delayed postcontrast T1W sequences were analyzed. The final decisions
112 for subject inclusion or exclusion were made by an ACVR board-certified radiologist (SS)
113 and a second-year ECVDI resident (AC).

114

115 MEDICAL RECORD DATA RECORDING:

116 Medical record entries were retrieved and evaluated by an ACVR board-certified radiologist
117 (SS) and a second-year ECVDI resident (AC). The reports of necropsy, surgical biopsy and/or
118 CSF analysis along with patients' age, sex, and breed were recorded. Because the aim of the
119 study was to describe the MRI features of brain abscesses and to compare them with ring-
120 enhancing gliomas in doubtful cases, the presence of MRI changes related to bite wounds
121 were recorded, but not considered as imaging criteria for including subjects in the study.

122

123 IMAGE ANALYSIS

124 Images were analyzed by an ACVR board-certified radiologist (SS), a ECVN board-certified
125 neurologist (MB) and a second-year ECVDI resident (AC) not blinded to the final diagnosis.
126 The final decision on the imaging characteristics was reached on a consensus basis. The
127 studies were randomly reviewed using a DICOM (i.e., Digital Imaging and Communications
128 in Medicine) viewer program (OsiriX DICOM viewer, Pixmeo, Geneva, Switzerland). The
129 three observers were asked to fill in a pre-defined standardized commercially available

130 spreadsheet (Microsoft Excel 2020, Microsoft, Redmond, Wash). The following MRI features
131 were assessed: T1W and T2W signal heterogeneity/homogeneity as well as the intensity
132 (hypo-, iso-, hyper-) of the signal compared to normal gray matter on the same sequences;
133 presence of a peripheral hypointense halo on T2W sequences compared to contents of the
134 lesion;¹³ presence of a T2 FLAIR attenuated component within the lesion; presence and grade
135 (0, no; 1, mild; 2, moderate; 3, severe) of perilesional white matter edema based on a
136 subjective evaluation; pattern of ring enhancement (even/uneven); presence of progressive
137 central enhancement on delayed post-contrast sequences (delayed post-contrast enhancement
138 was assessed in different planes if the same plane was not available)²⁹ and the ratio between
139 lesion diameter and maximum capsule thickness in the immediate T1 post contrast images. In
140 cases in which T2*W GE sequences, DWI or SWI were available, additional data were
141 collected such as the presence of susceptibility artifact (i.e., hemorrhage) and a hypointense
142 peripheral halo compared to lesion content in T2*W GE sequences;¹⁶ the presence of
143 abnormal diffusion restriction in DWI/ADC;^{18,21} the presence of “dual-rim sign” (defined as
144 two concentric rims at the margins of the lesion with the outer one being hypointense and the
145 inner one hyperintense relative to cavity contents) on SWI images as described previously.²⁰

146

147 STATISTICAL ANALYSIS

148 All analyses were performed with commercial software (MedCalc, Software Ltd, Ostend,
149 Belgium) by an experienced statistician (BC). Count data regarding the abscess/glioma
150 diagnosis were crossed referenced with the MRI findings to obtain contingency tables. Chi-
151 square test was applied to analyse data, using Yates correction for 2x2 contingency tables and
152 Fisher’s exact test when frequencies inside tables were less than 5. When a significant
153 association ($P < 0.05$) was found between an MRI qualitative predictor and abscess/glioma
154 classification, the relative risk and 95% confidence interval (95%CI) were calculated.

155 The ratio between the lesion diameter and capsule thickness in the immediate T1 post-contrast
156 sequences was analyzed using a receiver-operating characteristic (ROC) approach to identify
157 the cut-off that could best discriminate between abscesses and gliomas. The threshold was
158 calculated using the Youden criterion.³⁰

159

160 **RESULTS**

161 A total of 31 cases met the inclusion criteria. Sixteen patients were diagnosed with ring-
162 enhancing gliomas through necropsy (15/16) or surgical biopsies (1/15); Intra-axial abscesses
163 were diagnosed in 15 patients through necropsy (5/15), CSF analysis (7/15) and surgical
164 biopsies (3/15). Within the abscess group, 6/15 had evidence of bite wounds/penetrating
165 lesions visible as temporal muscle myopathy and calvarial focal defects in
166 continuity/contiguity with the intra-axial mass.

167

168 In the ring-enhancing glioma group there were 13 dogs and 3 cats. The canine breeds
169 represented in the study were Boxer (n = 3), French Bulldog (n = 2), Labrador Retriever (n =
170 2), Jack Russell terrier (n = 2), Lhasa Apso, Boston Terrier, Springer Spaniel and mixed-
171 breed (n = 1 each). Two Domestic short-haired and 1 Sacred Birman cat represented the feline
172 group. Of the 13 dogs, 6 were males (4 neutered) and 7 females (3 spayed). The 3 cats were 2
173 spayed females and 1 male. The median age was 8 years (range: 5-12) for dogs and 8 years
174 (range: 5-15) for cats.

175 In the intra-axial abscess group, there were 10 dogs (3 mixed-breed, 1 Boxer, 1 Staffordshire
176 Bull Terrier, 1 West Highland White Terrier, 1 Border Terrier, 1 Miniature Schnauzer, 1
177 Chihuahua and 1 Golden Retriever) and 5 cats (4 Domestic short-haired and 1 Domestic long-
178 haired cat). Of the 10 dogs 4 were males (1 neutered) and 6 females (3 spayed). The 5 cats
179 were 4 neutered males and 1 spayed female. The median age was 4 years old (range: 1-11) for

180 dogs and 9 years old (range: 5-12) for cats.

181

182 The MRI technical parameters for each institution are listed in Supplement 1 and 2,
183 respectively. The radiofrequency coil selections varied based on patient sizes and availability.
184 All the animals were imaged in sternal recumbency, under general anesthesia. MRI studies
185 were acquired with both low- and high-field MRI scanners. T2*W GE sequences were
186 available in 13 cases of ring-enhancing glioma and in 9 cases of intra-axial abscessation. DWI
187 sequences were obtained in 6 cases with ring-enhancing glioma and in one patient with a
188 brain abscess. SWI was available in only one patient with ring-enhancing glioma. Delayed
189 T1W post-contrast sequences performed at least 5 minutes after the first “immediate” post-
190 contrast sequence were available in 12 glioma cases and in 10 intra-axial abscess cases.

191

192 RING-ENHANCING GLIOMAS vs. BRAIN ABSCESSSES

193 MRI findings of ring-enhancing gliomas and brain abscesses are summarized in Table 1.
194 Comparisons between groups for MRI characteristics are provided in Table 2. Overall, brain
195 abscesses showed a more homogeneous signal on T1W and T2W sequences compared to
196 ring-enhancing gliomas. A peripheral hypointense halo on T2W and T2*W GE sequences
197 was significantly associated with brain abscesses rather than ring-enhancing gliomas (Figure
198 1). On postcontrast T1W sequences, abscesses showed a more even ring-enhancing capsule
199 compared to the ring-enhancing gliomas (figure 2), while ring-enhancing gliomas were more
200 likely to have a progressive central enhancement on T1W delayed postcontrast sequences
201 (figure 3). Based on the ROC analysis, a cut-off value of >12 in the ratio between lesion
202 diameter and capsule thickness in the immediate T1 post contrast sequences had a 43.75%
203 sensitivity and 85.71% specificity for the detection of ring-enhancing gliomas. The details of
204 the obtained measurements are provided in supplement 3. The intensity of the lesions

205 (hyperintense, isointense or hypointense) compared to the gray matter, the presence of a T2
206 FLAIR attenuating component within the mass, the presence and grade of T2 FLAIR
207 perilesional vasogenic edema, and the presence of intralesional susceptibility artefacts were
208 not statistically significant. The unrestricted or decreased diffusion in DWI/ADC sequence
209 was not statistically evaluated due to the low number of patients where this sequence was
210 available. However, 6/6 patients with ring-enhancing glioma and DWI/ADC available showed
211 unrestricted diffusion; whereas the lesion in the only patient with DWI/ADC available images
212 within the brain abscesses group was characterized by restriction to diffusion (figure 2).

213

214

215 **DISCUSSION**

216 Our study showed that ring-enhancing gliomas share several MRI features with intra-axial
217 brain abscesses. However, findings supported our first hypothesis in that some qualitative
218 MRI characteristics were significantly associated with brain abscess or ring-enhancing
219 glioma: a homogenous signal on T1W and T2W sequences, a T2W and T2*W GE peripheral
220 hypointense halo, and an even enhancing capsule were more likely associated with brain
221 abscesses. Progressive central enhancement on T1W delayed postcontrast sequences was
222 strongly associated with ring-enhancing gliomas while this feature was only present in a
223 single dog with a brain abscess. Findings also supported our second hypothesis in that a
224 threshold value of >12 for the ratio between lesion diameter and capsule thickness in T1 post-
225 contrast sequences was found to be a cut-off for discriminating between abscesses and
226 gliomas. The presence of bite wounds/penetrating lesions in continuity/contiguity with an
227 intra-axial mass makes a brain abscess the most likely differential diagnosis. However, we did
228 not consider them as imaging criteria because we aimed to focus on those MRI findings that
229 can help the clinician in a doubtful clinical situation.

230 In our cohort of patients, brain abscesses had a significantly more homogeneous signal on
231 T1W and T2W sequences, likely reflecting the presence of necrotic/fluid content in the
232 abscess.^{11-13,15,16} In contrast, ring-enhancing gliomas usually showed a more heterogeneous
233 T1W or T2W signal due to the presence of variable content in these tumors, including
234 hemorrhage, necrotic tumor tissue, cysts or altered cellular density.^{5-7,17,31}

235 There was absence of statistical significance in the evaluation of the type of T1W and T2W
236 signal compared to the grey matter in both gliomas and abscesses. This is related to the tumor
237 heterogeneity in gliomas and the variable ratio between cellular/protein content in abscesses
238 depending on their chronicity stage, respectively. During their development, abscesses begin
239 as a focal area of cerebritis histologically defined by a perivascular infiltration of neutrophils,
240 lymphocytes, and plasma cells within the brain parenchyma with an ill-defined central
241 necrotic zone composed of inflammatory cells, cellular debris, and microorganisms. In human
242 literature, cerebritis is used to denote brain parenchymal inflammation secondary to infection
243 with bacteria or other non-viral pathogens. In contrast, encephalitis is typically viral in
244 origin.³²

245 Subsequently, the necrotic center increases in size and becomes more well defined. As the
246 abscess becomes more chronic, the central necrotic area regresses and, if the patient survives
247 without treatment, the abscess will heal as a collapsed fibrotic glial scar.¹²

248 Our study demonstrates a significant correlation between a peripheral hypointense halo on
249 T2W and T2*W GE sequences and brain abscesses. This halo is due to paramagnetic free
250 radicals within phagocytic macrophages and it has already been described in both human and
251 veterinary medicine.^{8,13,15,16,19,21,33} However, although seen in most abscesses in our study, this
252 halo was not detected on all abscesses; moreover, it was also visible in the MRI study of one
253 patient with a glioma. A T2W and T2*W GE peripheral hypointense halo has been described
254 in both veterinary and human literature in several conditions such as gliomas, chronic

255 hematomas, metastases, granulomatous lesions, infarctions, meningiomas, and radiation
256 necrosis.^{12,19} Despite its statistical significance, it cannot therefore be regarded as
257 pathognomonic for brain abscesses.

258 Another MRI finding that statistically correlated with brain abscesses was the presence of an
259 even enhancing capsule. This may be explained by the pathophysiology of brain abscess
260 formation, which includes four different stages: the first two stages represent the “early” and
261 “late cerebritis” phases without collagenous capsule; during stage 3, called “early capsule”,
262 there is an initial deposition of collagen at the periphery of the necrotic center and it is
263 followed by ingrowth of granulation tissue and neovascularization; in the fourth or “late
264 capsule” stage there is complete formation of the capsule surrounding the necrotic center.¹²

265 Ring enhancing gliomas are not truly encapsulated, and the peripheral enhancing portion of
266 the lesion represents expanding neoplastic tissue with microvascular proliferations
267 surrounding a central necrotic core.³¹ The intrinsic neoplastic nature of this tissue may explain
268 both its uneven peripheral enhancement pattern and the progressive central enhancement
269 noted in 9 out of the 12 T1W delayed postcontrast sequences that correlated with ring-
270 enhancing gliomas. In both veterinary and human literature, intra-axial lesions usually show
271 progressively increased conspicuity on delayed postcontrast sequences.^{4,29,34} Moreover, the
272 presence of tumor angiogenesis along with poorly vascularized peripheral neoplastic tissue
273 surrounding the necrotic center may play a role in the delayed central progression of the
274 enhancement.³¹

275 In one brain abscess a very mild progressive central enhancement was seen. In this case,
276 immediate and delayed postcontrast T1W sequences were acquired in different planes and the
277 progressive central enhancement may therefore not be real. Other possible explanations
278 include a partial volume artifact due to the capsule’s thickness or the presence of a very thick
279 capsule that necessitated more time to enhance completely.

280 When evaluating the ratio between the lesion diameter and the capsule's thickness in the
281 immediate postcontrast T1W sequences, a cut-off >12 (43.75% sensitivity and 85.71%
282 specificity) can be proposed for the detection of ring-enhancing gliomas. The uneven
283 peripheral enhancement pattern of ring-enhancing gliomas due to the presence of
284 microvascular proliferation compared to the more even and smooth capsule of brain
285 abscesses^{12,31} would explain why ring-enhancing gliomas had higher lesion diameter:capsule
286 thickness ratio than abscesses.

287 T2 FLAIR sequences have been proposed to characterize fluid collections and differentiate
288 fluid-cavitary lesions from other parenchymal T2 high signal lesions.⁶ Cystic regions are
289 typical of canine glioblastoma but can also occur in approximately one-third of low-grade
290 canine gliomas;^{6,31} on the other hand, brain abscesses are associated with a necrotic core
291 during their development which may mimic the signal intensity and the cellular density of a
292 ring-enhancing glioma.^{12,31} This may explain the lack of statistical significance of an
293 intralesional T2 FLAIR attenuating component in our study.

294 The grade of the perilesional vasogenic edema was not statistically significant; vasogenic
295 edema is secondary to the disruption of the blood-brain-barrier (BBB) and represents a
296 nonspecific feature of several brain diseases including neoplastic and infectious disorders.^{35,36}

297 In humans, two patterns of vasogenic edema have been described: type 1 is seen in the
298 immediate vicinity of low-grade and nonglial tumors and is thought to be secondary to
299 parenchymal compression with secondary ischemia and necrosis; type 2 occurs with high-
300 grade glial tumors and is characterized by fingerlike projections reflecting tumor
301 microinvasion causing additional derangements of the BBB.³⁵ Further studies are needed to
302 investigate the relationship between the severity of perilesional vasogenic edema, brain
303 abscesses and low- and high-grade gliomas.

304 The presence of intralesional T2*W GE susceptibility artifact was observed in 4/13 patients
305 with ring-enhancing gliomas and only in 1/9 with brain abscesses, failing to achieve statistical
306 significance, probably due to the small sample of patients. These susceptibility artifacts were
307 likely consistent with hemorrhage, which is more commonly reported in gliomas.^{5-7,31,37} A
308 recent article in veterinary medicine recommends the use of SWI because it allows better
309 definition of intracranial hemorrhage.³⁷ In the same study, the presence of intra- and
310 extralesional fine, linear, and continuous susceptibility SWI artefacts was identified in 74.1%
311 of intracranial tumors and was interpreted as neovascularization.³⁷ In our study population,
312 SWI images were only available for a single glioma patient, showing some intralesional
313 foci/tubular susceptibility artifacts that were not visible on the T2*W GE sequence. In the
314 brain abscess group, T2*W GE intralesional susceptibility artifacts were seen in one feline
315 patient. These artifacts were attributed to hemorrhagic foci secondary to the recent bite wound
316 reported in the medical record.

317 Only seven MRI studies included a DWI/ADC sequence. This sequence was not included as
318 part of the standard MRI brain protocol for many of the institutions. All ring-enhancing
319 glioma patients for whom a DWI/ADC sequence was available (n=6), showed an unrestricted
320 diffusion of the lesion whereas the only patient with a brain abscess showed an abnormal
321 restriction to diffusion. These findings agree with what is reported in human and veterinary
322 medicine^{21,23, 33, 38,39} In humans, atypical diffusion (e.g., restriction to diffusion in gliomas and
323 unrestricted diffusion in brain abscess) is reported in 5-21% of the cases.²⁴⁻²⁶ In veterinary
324 medicine, restriction to diffusion in glial cell tumors has been described⁴⁰ while there are no
325 reports about unrestricted diffusion in brain abscesses.

326 In humans, the "dual rim sign" in SWI is the most specific imaging feature to distinguish
327 gliomas and abscesses.²⁰ This sign is typically seen in pyogenic abscesses while it has never
328 been reported in gliomas.²⁰ In our study, only one patient with glioma had SWI images

329 available, without evidence of “dual rim sign”. The lack of visualization of “dual rim sign” in
330 this patient agrees with what is reported in human medicine. Unfortunately, due to the
331 retrospective nature of our study, a SWI sequence was not included in the MRI protocol of
332 any patient of the abscess group. Future studies are needed to investigate the utility of the
333 SWI sequence in veterinary medicine.

334 The major limitation of this study is the use of different MRI equipment and protocols. Low-
335 field MRI might have failed in detecting small lesions. The different planes in some studies
336 between the immediate and the delayed postcontrast T1W sequences might have caused
337 incorrect interpretation of the effective progression of the central enhancement.

338 Another limitation is that, due to the retrospective and multicenter nature of the study over a
339 long period, different histological classification systems were used from different veterinary
340 pathologists with different backgrounds. For this reason, we decided not to make a distinction
341 between high- and low-grade ring-enhancing gliomas.

342 A potential source of bias was that the authors were aware of the final diagnosis at the time of
343 image interpretation. However, we did not consider it a major concern because the study
344 aimed to describe the MRI features of brain abscesses and ring-enhancing gliomas and not
345 test the diagnostic accuracy of MRI. In conclusion, even if several overlapping MRI features
346 between ring-enhancing gliomas and brain abscesses do exist, some features can help to
347 prioritize the MRI diagnosis. The presence of a homogeneous T1W or T2W signal intensity, a
348 T2W or T2*W GE peripheral hypointense halo and an even enhancing capsule may indicate a
349 brain abscess. The central progression of the enhancement on delayed postcontrast T1W
350 sequences is indicative of glial neoplasia. The addition of DWI and SWI sequences on high-
351 field MR scanners should be considered for assessment of intra-axial brain lesions which
352 cannot be easily discriminated using standard MRI sequences.

353

354 LIST OF AUTHOR CONTRIBUTIONS

355 Category 1

356 (a) Conception and Design: Swan Specchi, Andrea Carloni, Chiara Mattei, Marco Bernardini.

357 (b) Acquisition of Data: Andrea Carloni, Swan Specchi, Marco Bernardini, Chiara Mattei,

358 Angela Vittoria De Magistris, Francisco Llabres-Diaz, Jonathan Williams, Rodrigo Gutierrez-

359 Quintana, Anna Oevermann, Daniela Schweizer-Gorgas, Cyrielle Finck, Isabelle Masseur,

360 Valentina Lorenzo, Annalisa Sabatini.

361 (c) Analysis and Interpretation of Data: Andrea Carloni, Swan Specchi, Marco Bernardini,

362 Chiara Mattei, Barbara Contiero.

363

364 Category 2

365 (a) Drafting the Article: Andrea Carloni, Swan Specchi, Marco Bernardini, Chiara Mattei,

366 Barbara Contiero.

367 (b) Revising Article for Intellectual Content: Swan Specchi, Andrea Carloni, Marco

368 Bernardini, Chiara Mattei, Angela Vittoria De Magistris, Francisco Llabres-Diaz, Jonathan

369 Williams, Rodrigo Gutierrez-Quintana, Anna Oevermann, Daniela Schweizer-Gorgas,

370 Cyrielle Finck, Isabelle Masseur, Valentina Lorenzo, Annalisa Sabatini.

371

372 Category 3

373 (a) Final Approval of the Completed Article: Andrea Carloni, Swan Specchi, Marco

374 Bernardini, Chiara Mattei, Angela Vittoria De Magistris, Francisco Llabres-Diaz, Jonathan

375 Williams, Rodrigo Gutierrez-Quintana, Anna Oevermann, Daniela Schweizer-Gorgas,

376 Cyrielle Finck, Isabelle Masseur, Valentina Lorenzo, Annalisa Sabatini, Barbara Contiero.

377

378 Category 4

379 (a) Agreement to be accountable for all aspects of the work in ensuring that questions related

380 to the accuracy or integrity of any part of the work are appropriately investigated and

381 resolved: Andrea Carloni, Swan Specchi, Marco Bernardini, Chiara Mattei, Angela Vittoria

382 De Magistris, Francisco Llabres-Diaz, Jonathan Williams, Rodrigo Gutierrez-Quintana, Anna

383 Oevermann, Daniela Schweizer-Gorgas, Cyrielle Finck, Isabelle Masseau, Valentina Lorenzo,

384 Annalisa Sabatini, Barbara Contiero.

385 REFERENCES

- 386 1. Snyder JM, Shofer FS, Van Winkle TJ, Massicotte C. Canine Intracranial Primary
387 Neoplasia: 173 Cases (1986–2003). *J Vet Intern Med* 2006;20:669–75.
- 388 2. Song RB, Vite CH, Bradley CW, Cross JR. Postmortem Evaluation of 435 Cases of
389 Intracranial Neoplasia in Dogs and Relationship of Neoplasm with Breed, Age, and
390 Body Weight. *J Vet Intern Med* 2013;27:1143–52.
- 391 3. Troxel MT, Vite CH, Van Winkle TJ, et al. Feline Intracranial Neoplasia:
392 Retrospective Review of 160 Cases (1985–2001). *J Vet Intern Med* 2003;17:850–59.
- 393 4. Hecht S. Brain neoplasia. In: Mai W eds. *Diagnostic MRI in dogs and cats*, 1st ed.
394 Boca Raton, FL: CRC press;2018:211-40.
- 395 5. Wisner ER, Dickinson PJ, Higgins RJ. Magnetic resonance imaging features of canine
396 intracranial neoplasia. *Vet Radiol Ultrasound* 2011;52:S52–S61.
- 397 6. Bentley RT, Oberb CP, Andersonb KL, et al. Canine intracranial gliomas:
398 Relationship between magnetic resonance imaging criteria and tumor type and grade.
399 *Vet J* 2013:463–71.
- 400 7. Young BD, Levine JM, Porter BF. Magnetic resonance imaging features of
401 intracranial astrocytomas and oligodendrogliomas in dogs. *Vet Radiol Ultrasound*
402 2011;52:132–41.
- 403 8. Thomas WB. Nonneoplastic Disorders of the Brain. *Clin Tech Small Anim Pract*
404 1999;14:125–47.
- 405 9. Sonnevile R, Ruimy R, Benzonana N, et al. An update on bacterial brain abscess in
406 immunocompetent patients. *Clin Microbiol Infect* 2017;23:614–20.
- 407 10. Radaelli ST, Platt SR. Bacterial Meningoencephalomyelitis in Dogs: A Retrospective
408 Study of 23 Cases (1990–1999). *J Vet Intern Med* 2002;16:159–63.

- 409 11. Mateo I, Lorenzo V, Munoz A, Pumarola M. Brainstem Abscess Due to Plant Foreign
410 Body in a Dog. *J Vet Intern Med* 2007;21:535–38.
- 411 12. Klopp LS, Hathcock JT, Sorjonen DC. Magnetic resonance imaging features of brain
412 stem abscessation in two cats. *Vet Radiol Ultrasound* 2000;41:300-307.
- 413 13. Costanzo C, Garosi LS, Glass EN. Brain abscess in seven cats due to a bite wound:
414 MRI findings, surgical management and outcome. *J Feline Med Surg* 2011;13:672–80.
- 415 14. Rosenblatt AJ, Scrivani PV, Caserto BG et al. Imaging diagnosis –
416 meningoencephalitis secondary to suppurative rhinitis and meningoencephalocele
417 infection in a dog. *Vet Radiol Ultrasound* 2014;55:614–19.
- 418 15. Seiler G, Cizinauskas S, Scheidegger J, Lang L. Low-field magnetic resonance
419 imaging of a pyocephalus and a suspected brain abscess in a German Shepherd dog.
420 *Vet Radiol Ultrasound* 2001;42:417–22.
- 421 16. Bach JF, Mahony OM, Tidwell AS, Rush JE. Brain abscess and bacterial endocarditis
422 in a Kerry BlueTerrier with a history of immune-mediated thrombocytopenia. *J Vet*
423 *Emerg Crit Care* 2007;17:409–15.
- 424 17. Miller AD, Ryan Miller C, Rossmeisl JH. Canine Primary Intracranial Cancer: A
425 Clinicopathologic and Comparative Review of Glioma, Meningioma, and Choroid
426 Plexus Tumors. *Front Oncol* 2019; 9:1151. doi: 10.3389/fonc.2019.01151.
- 427 18. Huisman T. Tumor-like lesions of the brain. *Cancer Imaging* 2009;9: S10-S13.
- 428 19. Haimes BA, Zimmerman RD, Morgello S, et al. MR imaging of brain abscesses. *Am J*
429 *Roentgenol* 1989;152:1073–85.
- 430 20. Toh CH, Wei K-C, Chang C-N, et al. Differentiation of pyogenic brain abscesses from
431 necrotic glioblastomas with use of Susceptibility-Weighted Imaging. *Am J*
432 *Neuroradiol* 2012;33:1534–38.

- 433 21. Kim YJ, Chang K-H, Song IC, et al. Brain abscess and necrotic or cystic brain tumor:
434 discrimination with signal intensity on Diffusion Weighted MR Imaging. *Am J*
435 *Neuroradiol* 1998;171:1487–90.
- 436 22. Toh CH, Wei K-C, Ng S-H. Differentiation of brain abscesses from necrotic
437 glioblastomas and cystic metastatic brain tumors with diffusion tensor imaging. *Am J*
438 *Neuroradiol* 2011; 32:1646–51.
- 439 23. Chiang I-C, Hsieh T-J, Chiu M-L, et al. Distinction between pyogenic brain abscess
440 and necrotic brain tumour using 3-tesla MR spectroscopy, diffusion and perfusion
441 imaging. *Br J Radiol* 2009;82: 813–20.
- 442 24. Reddy JS, Mishra AM, Behari S, et al. The role of diffusion-weighted imaging in the
443 differential diagnosis of intracranial cystic mass lesions: a report of 147 lesions. *Surg*
444 *Neurol* 2006;66:246–51.
- 445 25. Reiche W, Schuchardt V, Hagen T et al. Differential diagnosis of intracranial ring
446 enhancing cystic mass lesions—Role of diffusion-weighted imaging (DWI) and
447 diffusion-tensor imaging (DTI). *Clin Neurol Neurosurg* 2010;112:218–25.
- 448 26. Hakyemez B, Erdogan C, Yildirim N, Parlak M. Glioblastoma multiforme with
449 atypical diffusion-weighted MR findings. *Br J Radiol* 2005;78:989–92.
- 450 27. Bersan E, Maddox T, Walmsley G, et al. CT-guided drainage of a brainstem abscess
451 in a cat as an emergency treatment procedure. *J Feline Med Surg Open Reports*.
452 January 2020. doi:10.1177/2055116919896111.
- 453 28. Bilderback AL, Faissler D. Surgical management of a canine intracranial abscess due
454 to a bite wound. *J Vet Emerg Crit Care* 2009; 19(5): 507–12.
- 455 29. Carmel EN, d’Anjou M-A, Blond L, Beauchamp G, Parent J. Effect of acquisition
456 time on observer variability and qualitative characterization of gadolinium-enhancing

- 457 brain lesions in dogs and cats. Abstracts from the annual meeting of the American
458 College of Veterinary Radiology. *Vet Radiol Ultrasound* 2010;51: 221-35.
- 459 30. Youden WJ."Index for rating diagnostic tests". *Cancer* 1950;3:32–35.
- 460 31. Lipsitz D, Higgins RJ, Kortz GD. Glioblastoma Multiforme: Clinical Findings,
461 Magnetic Resonance Imaging, and Pathology in Five Dogs. *Vet Pathol* 2003;40:659–
462 69.
- 463 32. Rath TJ, Hughes M, Arabi M, Shah GV. Imaging of Cerebritis, Encephalitis, and
464 Brain Abscess. *Neuroimag Clin N Am* 2012;22:585–607.
- 465 33. Nagendran A, McConnel JF. Diffusion- and perfusion-weighted imaging
466 characteristics of an intracranial abscess in a cat. *J Small Anim Pract.* 2021
467 Aug;62(8):714. doi: 10.1111/jsap.13322. Epub 2021 Mar 23. PMID: 33759197.
- 468 34. Song GJ, Chang K-H, Na DK, et al. Delayed Effect of Contrast Enhancement in Brain
469 Tumors on MRI. *J Korean Soc Radiol* 1995 32(3):383-88.
- 470 35. Ho M-L, Rojas R, Eisenberg RL. Cerebral Edema. *Am J Roentgenol* 2012;99:W258–
471 W273.
- 472 36. Patel K, Clifford DB. Bacterial Brain Abscess. *Neurohospitalist* 2014;4(4):196-204.
- 473 37. Weston P, Morales C, Dunning M, et al. Susceptibility weighted imaging at 1.5 Tesla
474 magnetic resonance imaging in dogs: Comparison with T2*-weighted gradient echo
475 sequence and its clinical indications. *Vet Radiol Ultrasound.* 2020;61:566–76.
- 476 38. Desprechins B, Stadnik T, Koerts G, et al. Use of Diffusion-Weighted MR Imaging in
477 Differential Diagnosis Between Intracerebral Necrotic Tumors and Cerebral
478 Abscesses. *Am J Neuroradiol* 1999;20:1252–57.
- 479 39. Scherf G, Sutherland-Smith J, and Uriarte A. Dogs and cats with presumed or
480 confirmed intracranial abscessation have low apparent diffusion coefficient values.
481 *Vet Radiol Ultrasound.* 2022; <https://doi.org/10.1111/vru.13064>.

482 40. Sutherland-Smith J, King R, Faissler D, et al. Magnetic resonance imaging apparent
483 diffusion coefficients for histologically confirmed intracranial lesions in dogs. *Vet*
484 *Radiol Ultrasound*. 2011;52:142–148.

485 Table 1: Qualitative MRI features of ring-enhancing gliomas and brain abscesses in dogs and
 486 cats.

			Glioma (n = 16)	Abscess (n = 15)
Signal homogeneity	T1W	Homogeneous	4/16 (25%)	10/15 (66%)
		Heterogeneous	12/16 (75%)	5/15 (33%)
	T2W	Homogeneous	0/16 (0%)	5/15 (33%)
		Heterogeneous	16/16 (100%)	10/15 (66%)
Signal intensity	T1W	Hypointense	11/16 (69%)	14/15 (93%)
		Isointense	4/16 (25%)	1/15 (6%)
		Hyperintense	1/16 (6%)	0/15 (0%)
	T2W	Hypointense	0/16 (0%)	3/15 (20%)
		Isointense	0/16 (0%)	1/15 (6%)
		Hyperintense	16/16 (100%)	11/15 (73%)
T2W peripheral hypointense halo	Presence	1/16 (6%)	9/15 (60%)	
	Absence	15/16 (93%)	6/15 (40%)	
T2*W GE peripheral hypointense halo	Presence	1/13 (8%)	5/9 (55%)	
	Absence	12/13 (92%)	4/9 (44%)	
T2 FLAIR intralesional attenuating component	Presence	10/16 (62%)	9/15 (60%)	
	Absence	6/16 (37%)	6/15 (40%)	
T2 FLAIR white matter perilesional edema	Grade 0-1	8/16 (50%)	2/15 (13%)	
	Grade 2-3	8/16 (50%)	13/15 (86%)	
Pattern of ring-enhancement	Even	1/16 (6%)	10/15 (66%)	
	Uneven	15/16 (93%)	5/15 (33%)	
Progressive central enhancement on delayed T1W post-contrast	Presence	9/12 (75%)	1/10 (10%)	
	Absence	3/12 (25%)	9/10 (90%)	
Susceptibility artifacts on T2*W GESWI	Presence	4/13 (31%)	1/9 (11%)	
	Absence	9/13 (69%)	8/9 (89%)	
Signal on DWI/ADC	Unrestricted diffusion	6/6 (100%)	0/1 (0%)	
	Decreased diffusion	0/6 (0%)	1/1 (100%)	
“Dual rim sign” on SWI	Presence	0/1 (0%)	N/A	
	Absence	1/1 (100%)	N/A	

487

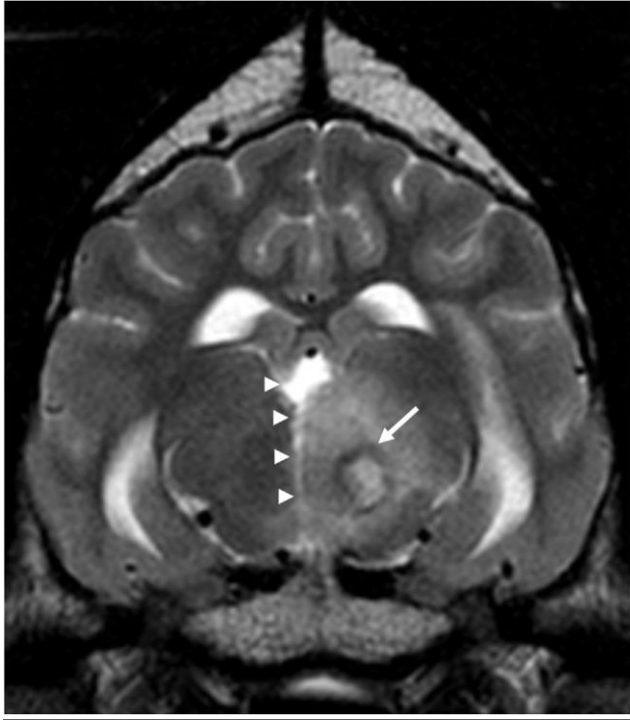
488

489

490

491 Table 2: Comparison between MRI findings in ring-enhancing gliomas and brain abscesses in
 492 dogs and cats.

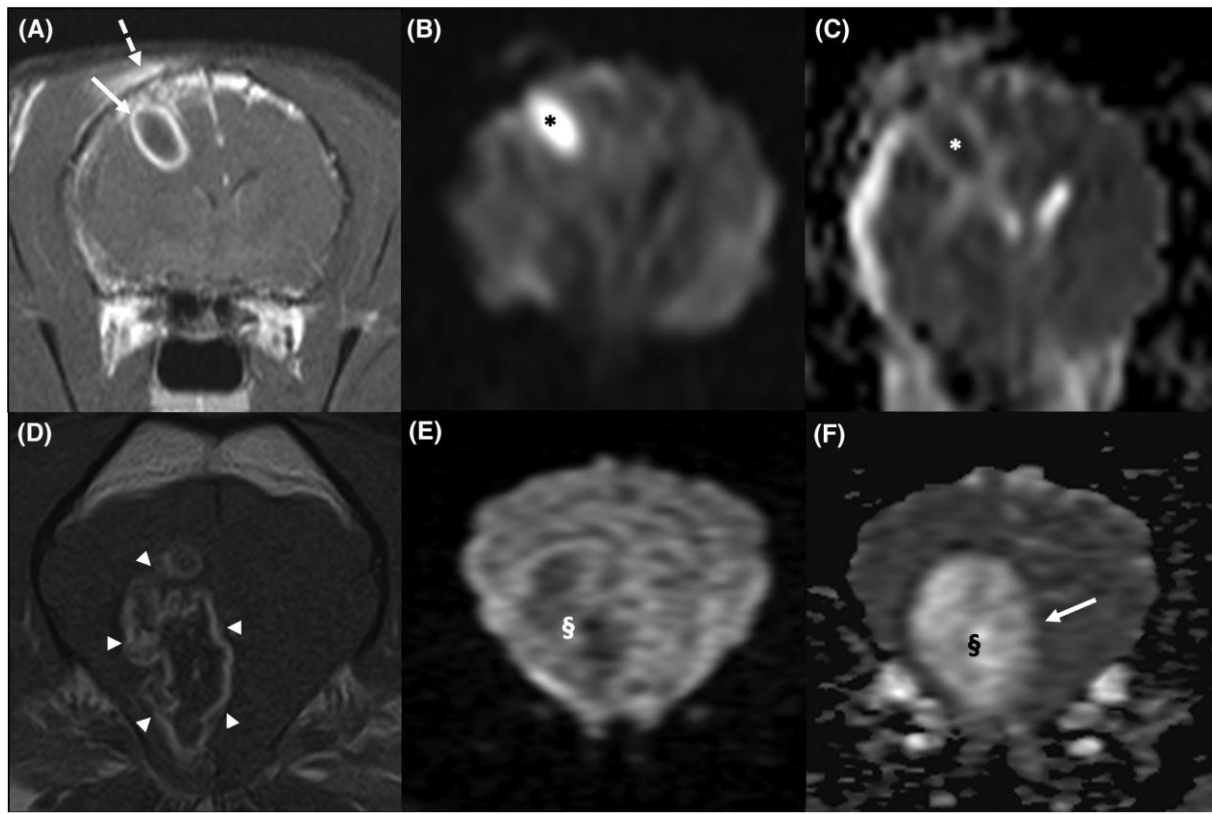
	Gliomas	Abscesses	Chi-square	P	Relative	95%CI
	N=16	N=15	test		risk	
T2W homogeneous lesion	0	5	4.13	0.042	2.6	1.6-4.23
T1W homogeneous lesion	4	10	3.87	0.049	2.4	1.08-5.45
Intensity of the lesion on T2W sequences			4.90	0.050		
- hyper	16	11	2.81	0.093		
- iso	0	1	0.001	0.974		
- hypo	0	3	1.62	0.202		
Intensity of the lesion on T1W sequences			3.13	0.251		
- hyper	1	0	0.001	0.974		
- iso	4	1	0.81	0.369		
- hypo	11	14	1.63	0.202		
T2 FLAIR intralesional attenuating component	10	9	0.05	0.821		
T2 FLAIR white matter perilesional edema			5.56	0.162		
- grade 2-3	8	13	3.23	0.072		
- grade 0-1	8	2	1.63	0.202		
Peripheral T2 hypointense halo	1	9	7.92	0.005	3.15	1.55-6.39
Peripheral T2*W GE hypointense halo	1	5	3.97	0.046	3.33	1.33-8.37
Susceptibility artifacts on T2*W GE sequences	4	1	0.32	0.572		
Even ring-enhancing pattern on T1W + C sequences	1	10	9.85	0.002	3.64	1.66-7.95
Progressive central enhancement on delayed T1W post-contrast	9	1	6.86	0.009	0.13	0.02-0.88



494

495 Figure 1: Transverse T2W FSE image (1.5 T, TR 2500, TE 15) of a one-year-old, neutered
496 male, American Staffordshire Terrier with left thalamic abscess. Note the peripheral
497 hypointense halo (arrow) surrounding a homogeneous hyperintense center. There is a
498 moderate mass effect on the third ventricle (arrowheads) along with moderate T2
499 hyperintense vasogenic edema surrounding the lesion.

500

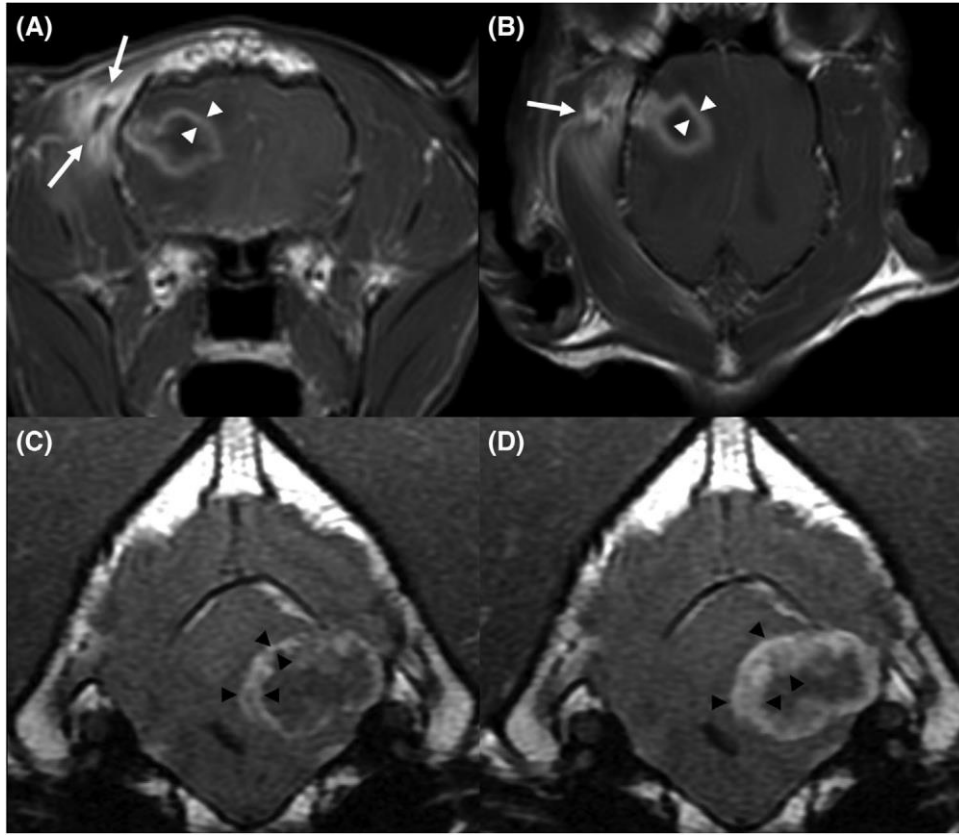


501

502 Figure 2: (A-C; 1.5 T, transverse T1W FSE TR 500, TE 13 and transverse DWI/ADC TR
 503 4233, TE 110, B value 1000) 9-year-old, male neutered, DSH cat with a right parietal lobe
 504 abscess secondary to a bite wound. An even, well-defined ring-enhancing lesion with
 505 hypointense center (arrow) is visible on the T1 post-contrast sequence (A); right temporal
 506 myopathy and a calvarial defect are also visible (dashed arrow). On the transverse DWI (B)
 507 the central portion of the abscess is strongly hyperintense to normal brain parenchyma (black
 508 asterisk) while it shows low values (white asterisk) on the ADC map (C), consistent with
 509 restriction to diffusion. (D-F; 1.5 T, transverse T1W FSE TR 465, TE 11 and transverse
 510 DWI/ADC TR 4288, TE 94, B value 1000) 5-year-old, male, French Bulldog with ring-
 511 enhancing glioma of the right fronto-parietal lobe. The T1W post-contrast sequence shows an
 512 unevenly marginated ring-enhancing glioma (arrowheads) (D). On the transverse DWI (E) the
 513 central portion of the lesion is hypointense (white §) to normal brain parenchyma while on the
 514 ADC map (F) it shows high signal (black §), consistent with unrestricted diffusion.

515 Note the difference between the even enhancing capsule of the brain abscess (A) compared to
516 the unevenly marginated ring-enhancing glioma (D).

517



518

519 Figure 3: Immediate post-contrast T1W transverse (A) and dorsal delayed post-contrast T1W
520 (B) images (1.5 T, transverse T1W FSE TR 500, TE 13) of a 9-year-old, male neutered, DLH
521 cat with a right temporo-parietal lobe abscess secondary to a bite wound with temporal
522 myopathy (arrows). Despite the different acquisition planes, the thickness of the abscess'
523 capsule does not increase over time (white arrowheads). Immediate post-contrast T1W
524 FLAIR (C) and delayed post-contrast T1W FLAIR (D) transverse images (1.5 T, transverse
525 T1W FLAIR FSE TR 2560, TE 26, TI 1013) of a 9-year-old, female spayed, Labrador
526 Retriever with a left cerebellar ring-enhancing glioma. Note the conspicuous central
527 progression (black arrowheads) of the enhancement on the delayed post-contrast sequence.